Ship Detection with Wireless Sensor Networks

Hanjiang Luo, *Student Member*, *IEEE*, Kaishun Wu, *Member*, *IEEE*, Zhongwen Guo, *Member*, *IEEE*, Lin Gu, *Member*, *IEEE*, and Lionel M. Ni, *Fellow*, *IEEE*

Abstract—Surveillance is a critical problem for harbor protection, border control or the security of commercial facilities. The effective protection of vast near-coast sea surfaces and busy harbor areas from intrusions of unauthorized marine vessels, such as pirates smugglers or, illegal fishermen is particularly challenging. In this paper, we present an innovative solution for ship intrusion detection. Equipped with three-axis accelerometer sensors, we deploy an experimental Wireless Sensor Network (WSN) on the sea's surface to detect ships. Using signal processing techniques and cooperative signal processing, we can detect any passing ships by distinguishing the ship-generated waves from the ocean waves. We design a three-tier intrusion detection system with which we propose to exploit spatial and temporal correlations of an intrusion to increase detection reliability. We conduct evaluations with real data collected in our initial experiments, and provide quantitative analysis of the detection system, such as the successful detection ratio, detection latency, and an estimation of an intruding vessel's velocity.

Index Terms—Ship detection, wireless sensor networks, target tracking, surveillance security, harbor protection.

1 Introduction

Intrusion detection on the sea is a critical surveillance problem for harbor protection, border security, and the protection of commercial facilities, such as oil platforms and fisheries. The traditional methods of detecting ships entail the use of radars or satellites which are very expensive. Besides the high cost, satellite images are easily affected by cloud cover, and it is difficult to detect small boats or ships on the sea with marine radar due to the noise or clutter generated by the uneven sea surface.

Terrestrial intrusion detection with Wireless Sensor Networks (WSNs) have recently been developed [1], [2], [3]. These networks deploy magnetometers, thermal sensors, and acoustic sensors in monitored areas to detect the presence of intruders [1], [4]. Though such networks may work well on the land, it is challenging to deploy these sensors on the sea surface for ship detection. The main challenge is that when sensors are deployed on the sea surface, they are not static and get tossed by ocean waves which makes them move around randomly [5]. The random movement of the node makes it difficult for most sensors to detect an intrusion. Due to stability requirements, camera sensors cannot work well either [6].

A V-shaped wake and its resulting waves is generated by a ship passing through the water [7]. Although the study of the ship-generated waves is an old topic, it mainly focused on reducing wave resistance through hull design, or preventing damage to coastal or floating marine structures [14], the investigation of the characteristics of ship waves propagated over large distances has not been the focus area in most of the research.

In this paper, we propose a novel approach: ship detection by taking advantage of the characteristics of ship-generated waves with WSNs. We have deployed an experimental WSN to detect ships by using three-axis accelerometer sensors with iMote2 on buoys on the sea surface. Using signal processing, we observed that ocean waves and ship-generated waves have different energy spectrums. We designed a three-tier intrusion detection system to detect intruding vessels. In the system, we propose to exploit spatial and temporal correlations of an intrusion to increase detection reliability. We conducted evaluations with real data collected by our initial experiments, and provide analysis of the detection system, such as the successful detection ratio and detection latency. To the best of our knowledge, this is the first detailed, systematic experimental study of ship intrusion detection with WSNs.

The paper is organized as follow: in Section 2, we discuss how to distinguish between ship-generated waves and ocean waves. The design of the three-tier detection system is presented in Section 3. In Section 4, we provide the performance evaluation. We survey the related work in Section 5. Finally, we present our conclusions and make suggestions for future research in Section 6.

- *H. Luo is with the Department of Information Engineering, Zibo Vocational Institute, Liantong Road, Zibo 255314, China. E-mail: fluo.wirelessg@gmail.com.*
- *K. Wu is with the School of Physics and Engineering, National Engineering Research Center of Digital Life, Sun Yat-sen University, Guangzhou, China, and the Fok Ying Tung Graduate School, The Hong Kong University of Science and Technology, Hong Kong. E-mail: kwinson@ust.hk.*
- *Z. Guo is with the Department of Computer Science, Ocean University of China, 5 Yushan Road, Qingdao 266003, China. E-mail: fguozhwg@ouc.edu.cn.*
- *L. Gu and L.M. Ni are with the Department of Computer Science and Engineering, The Hong Kong University of Science and Technology, Hong Kong. E-mail: {lingu, ni}@cse.ust.hk.*

Manuscript received 24 Feb. 2011; revised 3 Oct. 2011; accepted 8 Oct. 2011; published online 16 Nov. 2011.
Recommended for acceptance by Y.-C. Tseng.
For information on obtaining reprints of this article, please send e-mail to: tpds@computer.org, and reference IEEECS Log Number TPDS-2011-02-0111.
Digital Object Identifier no. 10.1109/TPDS.2011.274.

Fig. 1. Wake and resulting waves generated by a passing boat.

2 Distinguish Between Ship-Generated Waves and Ocean Waves

As mentioned in Section 1, node movement on the sea surface makes it hard to detect an intrusion target. Observing ship-generated waves, as shown in Fig. 1, we intend to detect ships by detecting the ship's waves.

2.1 Ship Wave Patterns and Wave Dissipation

When a ship moves across a surface of water, it generates waves which comprise divergent and transverse waves as shown in Fig. 2. Kelvin found that V-shaped patterns were formed by two locus of cusps whose angle with the sailing line is $19°28'$ in deep water [7], and the angle between the sailing line and the diverging wave crest lines at the cusp locus line should be $54°44'$. Note that this pattern is independent of the size and velocity of the ship.

When the ship's waves spread out sideways and propagate from the sailing line, both the height and energy of the waves decrease. The research in [15] pointed out that the transverse waves decrease inversely proportional to the square root of the distance from the vessel, which means that transverse waves decline much faster than divergent waves. In addition, when we observe ship-generated waves at a fixed spatial point, the ship-generated wave train has a limited duration [16].

The maximum wave height H_m at distance d from the sailing line can be expressed as the following equation:

$$H_m = cd^{-\frac{1}{3}}, \tag{1}$$

where c is a parameter related to the speed of the passing ship. The speed of the ship-wave W_v can be predicted by the following equation:

$$W_v = V \times cos\Theta, \tag{2}$$

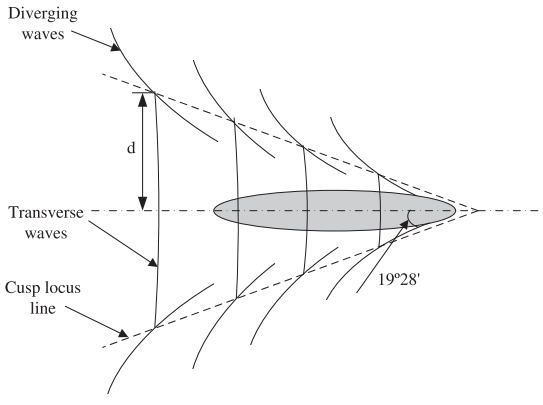

Fig. 2. Ship-generated wave model.

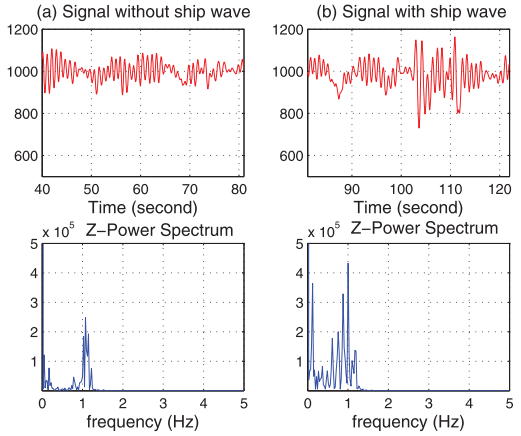

Fig. 3. Short-time Fourier transform. (a) Signal without ships and its spectrum. (b) Signal with ships and its spectrum.

where V is the speed of the ship, and $\Theta = 35.27(1 - e^{12(F_d - 1)})$ (F_d is the Froude number related to the traveling ship).

2.2 Measure Waves with Accelerometers and the Spectrum of the Ship Waves

The old method of measuring ship-generated waves is to measure the pressure fluctuations at some elevation points in the water column, then transform the pressure into wave height [16]. However, this method requires expensive equipment. In addition, it is difficult to deploy the devices underwater. In this paper, we use accelerometers to measure the actual surface movement of ship-generated waves. When the accelerometer is used in an ocean environment, the buoy and the accelerometer undergo a generally oscillatory, sinusoidal-like vertical acceleration due to wave action. The details of the experimental setup are in the supplemental files, which can be found on the Computer Society Digital Library at http://doi.ieeecomputersociety.org/10.1109/TPDS.2011.274.

In order to distinguish between ship-generated waves and ocean waves, we use Short Time Fourier Transform (STFT) to process the measured signals [17]. With 2,048 point sample STFT (40.96 s), we observe that ship-generated waves and normal ocean waves have a different energy spectrum as shown in Fig. 3. Fig. 3a shows ocean waves without ship waves. Its spectrum has a high, single peak concentration around a characteristic period around 1 Hz. On the contrary, the spectrum of the ocean waves combined with the ship waves, as shown in Fig. 3b, has multiple peaks and wide crests without distinct peaks.

3 Ship Intrusion Detection System Design

In this section, we first present the architecture of the distributed intrusion detection system, then discuss the three-tier intrusion system in detail.

3.1 The Architecture of the Intrusion Detection System

A reliable intrusion detection system may involve node-level detection, cluster-level classification, and sink-level classification.

The node-level detection involves sampling the event and extracting features. Once the node detects a target, it

is better that only the extracted features are transmitted to the local head node or a sink for further signal processing and classification, due to the energy constraints of the sensor node and the limitations of the communication bandwidth.

Cluster-level classification deals with more complicated tasks, such as Collaborative Signal Processing (CSP) or regional data fusion. The clusters are formed according to the geographical locations of nodes or the migration of the external "event" after the network deployment [3], [6]. In each cluster, a local head node takes charge of the data fusion or other coordination tasks within the cluster.

Sink-level detection involves processing the data sent from local head nodes, and the final decision will be reported to the external user via satellite or other means.

To deploy a real long-term intrusion detection surveillance system, some power management should be used [19]. To avoid the need for expensive periodic battery changes, the nodes may need expensive solar panel or other perpetual-powering solutions. Meanwhile some middleware services should be considered, such as the location of nodes, time synchronization, and routing infrastructure, etc., [1], [18], [19].

Next, we present the three-tier detection in detail.

3.2 Node-Level Detection

At node-level detection, the task for a single node is to detect ship waves generated by a nearby passing ship. In order to do that, the individual node periodically samples the event and processes the sampled data to extract features for node-level detection. In our scheme, the node first samples for a period of time after being deployed, then filters out any frequencies above 1 Hz.

Since the z-accelerometer signal fluctuates around $1g$, we deduct this value and let the signal fluctuates around zero. Before computing the average and standard deviation, we have the absolute value of those signals below zero. The reason being that, when the ship's waves disturb the buoy, all fluctuations either above $1g$ or below $1g$ contain the disturbance information.

We assume the sample signal value at time t is a_i, the total number of sampling points in time period T is u. The average sample value of this period T and the standard deviation can be computed as follows:

$$\begin{cases} m_{\Delta t} = \frac{1}{u}\sum_{i=1}^{u} a_i, \\ d_{\Delta t} = \sqrt{\frac{1}{u}\sum_{i=1}^{u}(a_i - m_{\Delta t})^2}. \end{cases} \tag{3}$$

Since ocean waves change with wind and time, the threshold should reflect those changes. Thus, we design an environment adaptive threshold by moving the average value and the standard deviation with time. The moving average and the standard deviation is defined as follows:

$$\begin{cases} m'_T = \beta_1 \times m_T + m_{\Delta t} \times (1 - \beta_1), \\ d'_T = \beta_2 \times d_T + d_{\Delta t} \times (1 - \beta_2), \end{cases} \tag{4}$$

where $m_{\Delta t}$ and $d_{\Delta t}$ are the historical average and the standard deviation, β_1 and β_2 are parameters which are empirically determined to 0.99 here.

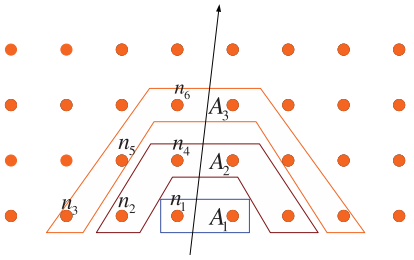

Fig. 4. Spatial and temporal correlation.

We define D_i for each sampled signal a_i as follows:

$$D_i = |a_i - d'_T|. \tag{5}$$

The threshold is defined as $D_{max} = Mm'_T$, where $M = 1, 2, 3$. If $D_i > D_{max}$, we consider that the threshold has been crossed.

Since the ship waves are actually a train of waves, the disturbance to the sensor should only last for a short period of time. In other words, the crossing of the threshold occurs several times within a short period of time Δt. Thus, we define anomaly frequency a_f as follows:

$$a_f = \frac{NA_{\Delta t}}{N_{\Delta t}}, \tag{6}$$

where $NA_{\Delta t}$ is the number of the crossing occurring during that period of time Δt, $N_{\Delta t}$ is the total number of samples within time period Δt.

The average energy of crossing within the period of time Δt can be computed as follows:

$$E_{\Delta t} = \frac{1}{NA_{\Delta t}}\sum_{\Delta t} {D_i}^2 \quad (D_i > D_{max}). \tag{7}$$

The node reports the detection to a local head node for further signal processing if a_f passes a predefined threshold, and it reports E_Δ and the onset time when the signal first exceeds the threshold.

3.3 Cluster-Level Detection

Though a passing ship can be detected by an individual node, many factors affect the detection results. For example, wind may affect the sensors and cause a flurry of false positives by directly moving sensors. Animals such as birds or fish may also disrupt the sensor readings. In addition, some nodes with hardware errors may not detect the ship when it is passing. Even with perfect detection, its positive report may not be transmitted back in a timely fashion due to wireless communication errors [21] and possible network congestions [20].

To improve the detection performance and decrease the false positive rate, it is useful that multiple nodes cooperatively detect the ship. In this section, we first present in-network data processing with spatial and temporal correlations between nodes, and then estimate the speed of a passing ship.

3.3.1 Spatial and Temporal Correlations

When a ship travels through a monitored area, it will continuously disturb a succession of small areas. As shown in Fig. 4, when a ship travels through the sensor networks, the waves generated by the passing ship disturb

the sensor areas A_1, A_2, A_3 in a sequential manner. These areas have spatial and temporal correlations. By exploiting these correlations, we can improve the reliability of the detection system.

In order to monitor the entire deployed area, the network should be partitioned into "cells" by forming static clusters. In this paper, we propose combining temporary clusters with these static clusters. The static clusters are formed according to the geographical location of the nodes, and we also set up temporary clusters on demand when a node's alarm is trigger. Since the nodes positions are fixed, they know where their neighbors are located. When a node discovers a ship intrusion, it initiates a temporary cluster, informs its neighboring nodes within N hops and automatically becomes the temporary cluster head.

If more than one node detects a ship intrusion before it receives detection signals from other nodes, the nodes contend to become the temporary cluster head. To simplify the process, when the nodes try to set themselves up as cluster heads, they could also send out their average detection energy, thus the node with the higher detection energy becomes the cluster head.

If the nodes within the cluster also find the intrusion, they report the findings to the temporary cluster head. If the cluster head has not received any report within a certain period of time, it will cancel the temporary cluster because its positive finding may be a false alarm. However, if it receives enough positive reports in a timely fashion, it will process the received data using the spatial and temporal correlations of the ship waves.

The ship will disturb nodes in several rows or columns just as Fig. 4 shows. Since the nodes nearest to the ship's travel line get a stronger signal strength than the other nodes in each row, all the disturbed nodes can be separated into two sides. For simplicity, we only consider one side of the nodes below.

In each row, we assume that the total number of active nodes (the node which has positive reports) is n. We define $C_{rt(i)}$ as the time correlations in row i. Because the cluster head knows the positions of each node, we arrange all reports according to their position and reporting time. For example, in row i, if and only if node $a's$ position is closer to the ship travel line and the reporting time is earlier than node $b's$, we order them. If the number of ordered reports is N, $C_{rt(i)}$ is computed as follows:

$$C_{rt(i)} = \frac{N}{n}, \tag{8}$$

where $C_{rt(i)} = 1$, if there is only one report in one row.

The group's time correlations C_{Nt} defines as follows:

$$C_{Nt} = \prod C_{rt(i)}, \tag{9}$$

where $C_{rt(i)}$ is the time correlations in each row.

$C_{re(i)}$ describes the energy correlations of reports in each row. Because the ship waves attenuate with distance between the ship travel line and the sensor, the nodes closer to the travel line have higher ship-wave energy. This will lead to different average energy $E_{\Delta t}$. We order all reports according to their positions and average energy. For example, in row i, if and only if node $a's$ position is closer to the ship travel line than node b, and $E_{\Delta t}(a) > E_{\Delta t}(b)$, we order them. If the number of sorted reports is N, $C_{re(i)}$ is defined as follows:

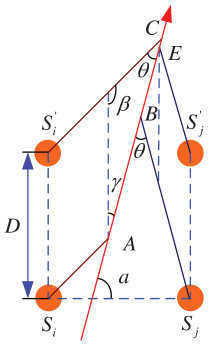

Fig. 5. Ship speed estimation.

$$C_{re(i)} = \frac{N}{n}, \tag{10}$$

where $C_{re(i)} = 1$, if there is only one report in one row.

C_{Ne} describes the cluster's energy correlations and is defined as follows:

$$C_{Ne} = \prod C_{re(i)}, \tag{11}$$

where $C_{re(i)}$ is the energy correlations in each row.

The correlation coefficient C measures the spatial and temporal correlations in a cluster and is defined as follows:

$$C = C_{Nt} \times C_{Ne}. \tag{12}$$

If C is greater than a threshold, the collected data are considered to have correlations. Then, the temporal cluster head reports the result to its static cluster head, and the cluster head will eventually reports the detection to the sink.

3.3.2 The Ship Speed Estimation

As described in Section 2, the angle between the locus of cusps and the sailing line is a fixed constant. Via this characteristic and the multinode correlated information collected by the temporary cluster head, we can estimate the speed of the intruding ship.

Fig. 5 shows the four nodes which involve the speed estimation. Detailed proof is provided in the online supplemental file, we only present the estimated speed of the ship v as the following equation:

$$\begin{cases} v = \dfrac{Dsin(\alpha - 70^\circ)}{(t_4 - t_3)sin\theta}, \\ \alpha = \arctan\left(\dfrac{t_2 + t_4 - t_1 - t_3}{t_2 + t_3 - t_1 - t_4}\tan 70^\circ\right), \end{cases} \tag{13}$$

where θ is 20°.

As for the direction of the ship, that is easy to obtain with the timestamps of the four nodes.

3.4 Sink-Level Detection

Though cluster-level detection increases the reliability of the intrusion detection, the sink-level detection has global knowledge of the whole network via cluster heads' reports, thus it can further reduce false alarms with the global view of spatial and temporal correlations of tracking reports.

Fig. 6. Experimental sensor network deployment.

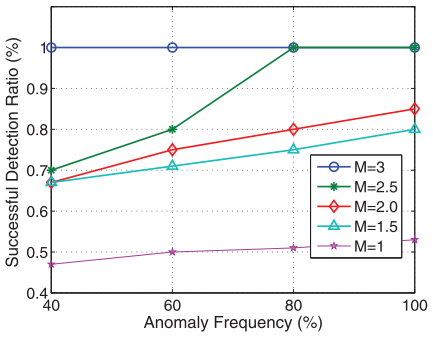

Fig. 7. The relationship between anomaly frequency and success detection ratio.

Since in most cases the intruding ship will keep moving, it will eventually move away from the monitored area. So if a target only affects several clusters and then disappears, it is most certainly a false alarm. For the same reason, if the sink receives many reports from a very large area or even the whole area in a very short period of time, the reason may be a strong wind or some of the networks' parameters are not set correctly. If bad weather comes suddenly, the accelerometers' signals will be abnormal. With global information available at the sink, it is easy to filter out these types of false alarms.

However, if the intruding ship stops periodically moving, it will make the detection more difficult. To deal with such a problem, we may make the cluster smaller to increase the number of clusters disturbed by the ship's intrusion. To distinguish between friend and foe ships, we may add ID to friendly ships. When such ships come, the system will not sound intrusion alarms. Another task for the sink-level detection is multitarget detection. Since the sink has the knowledge of the whole monitoring network, it is easy to monitor several intrusion targets at the same time. The sink may record reports which happen simultaneously in different geographical areas over large distances.

3.5 The Algorithm

An intrusion detection algorithm should include node and sink algorithms. For simplicity, we only present the node's algorithm SID in this paper. The algorithm includes initialization of node, intrusion detection, temporary cluster setup, correlation of spatial, and temporal data processing. The detailed algorithm is presented in the online supplemental file.

4 Performance Evaluation

In this section, we evaluate the detection system and provide analysis based on the real data which we collected in our initial experiments as shown in Fig. 6.

The experimental system is with 30 nodes deployed in a grid fashion as Fig. 4 shows, five nodes in a row and a total of six rows. The node's deployment distance D is 25 m. The ship travels along one side of the deployed area with three speed levels about 10, 16, and 20 knots, and with each speed the test runs 10 rounds. A more detailed description of the experiments are in the online supplemental files.

4.1 Node-Level Evaluation

In node-level evaluation, we evaluate the successful detection ratio of a node as shown in Fig. 7. From the figure, we observed that as the anomaly frequency a_f increases, the successful detection ratio also increases. This is because the anomaly frequency reflects the disturbance level of the ship's wake.

If we fix the anomaly frequency, as M increases, the successful detection ratio will increase. This is because if the threshold is higher, the noise of the ocean waves has less impact on the detection, thus the successful detection ratio of each node is improved. Owing to the noise of the ocean, the detection accuracy of each node is not very high. Thus, our design does not depend too much on the detection accuracy of individual nodes.

Observed from the figure, when $M = 2$ and $a_f = 60\%$, the successful detection ratio is above 70%. With more nodes cooperating to detect a ship's waves, the node-level detection ratio is sufficient to guarantee a successful cluster-level detection, which we discuss in Section 4.2.

4.2 Cluster-Level Evaluation

In culster-level evaluation, we evaluate the impact of correlation coefficient C and estimate the speed of an intruding ship.

4.2.1 The Impact of Correlations Coefficient C

We evaluate the sampled data with and without ship intrusions. We process five nodes' data in each row and compute correlation coefficient C from 4 to 6 rows, respectively, with a different M. As for ship intrusions of ships travelling at different speeds, we compute the correlation coefficient for each speed, and then average the coefficient.

The results are presented in Tables 1 and 2. Table 1 shows that there are false alarm reports when there is no ship intrusion. However, the data have a very low correlation coefficient C.

Compared with Table 1, Table 2 shows that the data have higher spatial and temporal correlations C with ship

TABLE 1
The Correlation Coefficient without Ship Intrusion

M	row=4	row=5	row=6
1	0.019	0.013	0.006
2	0.009	0.005	0.001
3	0.002	0	0

TABLE 2
The Correlation Coefficient with Ship Intrusion

M	row=4	row=5	row=6
1	0.62	0.53	0.47
2	0.75	0.69	0.60
3	0.81	0.72	0.68

intrusions. The results also reveal that as M increases, C also increases because more false positive reports will be filtered out.

Summarized from Tables 1 and 2, if the cluster consists of at least four rows of nodes, the cluster head can report the detection to the sink when the correlation coefficient C exceeds 0.4.

4.2.2 Ship Speed Estimation

To evaluate the ship speed estimation, we choose four deployed nodes as Fig. 5 shows. The ship uses two speeds of about 10 and 16 knots, respectively. With each speed the test runs 10 rounds, and the ship travels through the network at different angles and speeds to generate data. We only record the reports which have the highest detected energy within the test period. Then, we use (13) to compute the speed of the ship.

Fig. 8 shows the actual speed of the ship and the estimated speed of the ship. For the 10 knot test, the computed speed of the ship is between 8 and 12 knots. As for the 16 knot test, the figure is from 15 to 18 knots. There are two reasons for the estimated speed errors: first, the ship is not really traveling in a straight line due to the sea waves. Second, the nodes deployed in the sea are not static and have about a 2 m free drifting radius.

4.3 Sink-Level Evaluation

At sink-level detection, we mainly evaluate the detection latency and the relationship between ship speed and the successful detection ratio. The detection latency is shown in Fig. 9. Generally, the detection latency is decided largely by the speed of the intruding ship. As the ship's speed increases, the latency decreases sharply because the speed of the ship's wake is related to the speed of the ship, as shown in (2). The figure also shows, as more rows of nodes are included in the classification, the latency increases.

Fig. 10 shows the relationship between a successful detection ratio and the speed of the ship. We compare the

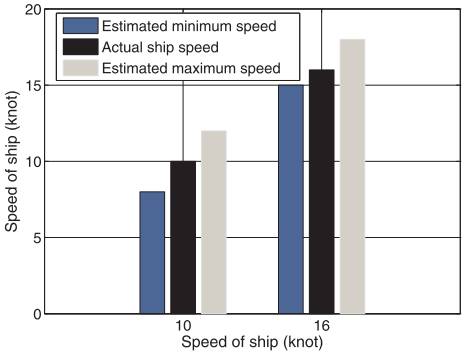

Fig. 8. Ship speed estimation.

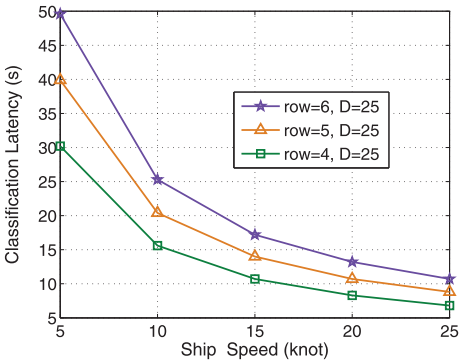

Fig. 9. Ship speed and classification latency.

results of different deployment distances, such as 25 and 50 m. The figure shows that as the ship speed increases, the successful detection ratio also increases. The reason is that the higher the ship's speed, the higher the ship-wave energy which is easier to detect with higher probability.

The figure also shows that as the node deployment distance increases, the successful detection ratio decreases sharply. This means that in order to have a high successful detection ratio, the node should not have been deployed too far.

5 Related Work

There is numerous research for terrestrial intrusion detection, classification, and target tracking [8], [9], [10], [11], [12], [13], in which magnetometers, thermal sensors, or acoustic sensors are deployed in a monitored area to detect intruders [22], [23], [24]. Some researchers have also deployed a number of successful real-world systems [1], [2], [3]. However, the sensors are mostly static after deployment, and as mentioned in Section 1, when sensors are deployed on the sea surface, they move randomly tossed by ocean waves which makes it difficult for most sensors to detect intrusion targets.

There is a small amount of research dealing with intrusion detection on the water. In [25], Carapezza et al. describe a coastal sensor network to detect, classify, and track submerged objects that may pose a threat. The unattended in-water sensors first perform the initial and coarse target detection, then the shore-based optical sensors develop refined tracks on the targets. Bunin et al. [26] developed an experiment on the Hudson River Estuary to detect ships.

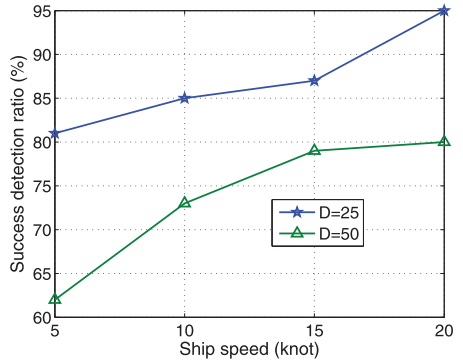

Fig. 10. Ship speed and successful detection ratio.

Their system combines a specialized prototype video system and a passive underwater acoustic sensor network to track and classify ships on the river. However, these are shore-based ship detection schemes. Our scheme can be entirely deployed in the water, and we leverage the movement of sensors by deploying accelerometers onto the sea surface to detect passing ships. We also exploit the spatial and temporal characteristics of the ship's wake to increase the detection reliability.

6 Conclusions and Future Work

In this paper, we present a three-tier ocean intrusion detection system by using accelerometer sensors to detect intrusion ships. We also exploit the spatial and temporal correlations of the intrusion to increase the detection reliability. We conducted evaluations with real data collected by our initial experiments, and provide analysis of the system.

Compared with traditional ship detection methods which can monitor a large area (e.g., radars or satellites) but cost a lot, our methods can be cheaper. Moreover, the satellites cannot perform real-time monitoring. With radar, we need some place to set up the equipment, and it is difficult to detect small boats. The schemes with WSNs are cheaper and can be deployed almost everywhere we want. More importantly, it can perform situ real-time monitoring, and provide more information of the monitored targets.

The main limitation of our scheme is that it requires a relatively dense network (cost more because the nodes are expensive now), especially to achieve a high detection ratio with small boats because of the high noise on the sea. Deploying a monitoring belt as in [2] and [4] may decrease the total number of deployed nodes. Combining with other sensors, such as acoustic sensors, may also help decrease the deployment density because sound travels far in the water. The algorithm is based on a grid deployed network, and it is better to deploy the sensor networks randomly in a real deployed system, like dropping buoys from a plane. However, it is more difficult than the grid network, and we leave it as our future work.

Meanwhile, we need further research on power management. In sink level detection, we should deal with ships which are trying to penetrate the invasion detection area using varying course, and traveling at different speeds to evade detection. The ship speed estimation also needs to be improved with intrusion vessels traveling at varying speeds and courses in the detection zone. Though the algorithm can detect multiple ships traveling along distances in different geographical areas, we need further research on multiple ships crossing the sensor region in close proximity to each other. The current design cannot support online intrusion detection, and we leave it as our future work.

Acknowledgments

This research was supported by the Project of Shandong Province Higher Educational Science and Technology Program No. J11LG88, the 2012 Guangzhou Pearl River New Star Technology Training Project, China NSFC Grants 60873248, 60933011, and 60933012, Hong Kong RGC Grants 617908 and 617710. The preliminary results of this paper were published in the proceedings of the IEEE ICDCS 2011. Kaishun Wu is the corresponding author of this paper.

References

[1] L. Gu et al., "Lightweight Detection and Classification for Wireless Sensor Networks in Realistic Environments," *Proc. Third Int'l Conf. Embedded Networked Sensor Systems (SenSys '05)*, pp. 205-217, 2005.

[2] A. Arora et al., "A Line in the Sand: A Wireless Sensor Network for Target Detection, Classification, and Tracking," *Computer Networks*, vol. 46, no. 5, pp. 605-634, 2004.

[3] M. Duarte and Y. Hen Hu, "Vehicle Classification in Distributed Sensor Networks," *J. Parallel and Distributed Computing*, vol. 64, no. 7, pp. 826-838, 2004.

[4] S. Kumar, T. Lai, and A. Arora, "Barrier Coverage with Wireless Sensors," *Proc. MobiCom*, pp. 284-298, 2005.

[5] Z. Yang, M. Li, and Y. Liu, "Sea Depth Measurement with Restricted Floating Sensors," *Proc. IEEE 28th Int'l Real-Time Systems Symp. (RTSS '07)*, pp. 469-478, 2007.

[6] B. Malhotra, I. Nikolaidis, and J. Harms, "Distributed Classification of Acoustic Targets in Wireless Audio-Sensor Networks," *Computer Networks*, vol. 52, no. 13, pp. 2582-2593, 2008.

[7] F. Ursell, "On Kelvin's Ship-Wave Pattern," *J. Fluid Mechanics Digital Archive*, vol. 8, no. 3, pp. 418-431, 2006.

[8] Z. Wang, E. Bulut, and B.K. Szymanski, "Distributed Energy-Efficient Target Tracking with Binary Sensor Networks," *ACM Trans. Sensor Networks (TOSN)*, vol. 6, no. 4, pp. 1-32, 2010.

[9] M. Arik and O.B. Akan, "Collaborative Mobile Target Imaging in UWB Wireless Radar Sensor Networks," *IEEE J. Selected Areas in Comm.*, vol. 28, no. 6, pp. 950-961, Aug. 2010.

[10] O. Garcia, A. Quintero, and S. Pierre, "A Global Profile-Based Algorithm for Energy Minimization in Object Tracking Sensor Networks," *Computer Comm.*, vol. 33, no. 6, pp. 736-744, 2010.

[11] V. Katiyar, P. Kumar, and N. Chand, "An Intelligent Transportation Systems Architecture Using Wireless Sensor Networks," *Int'l J. Computer Applications*, vol. 14, no. 2, pp. 22-26, 2011.

[12] Y.E.M. Hamouda and C. Phillips, "Metadata Based, Optimal Sensor Selection for Multi-Target Tracking in Wireless Sensor Networks," *Int'l J. Research and Rev. in Computer Science*, vol. 2, no. 1, pp. 189-200, 2011.

[13] C.C. Ooi and C. Schindelhauer, "Utilising Coverage Holes and Wireless Relays for Mobile Target Tracking," *Int'l J. Ad Hoc and Ubiquitous Computing*, vol. 7, no. 1, pp. 38-53, 2011.

[14] A. Velegrakis, M. Vousdoukasa, A. Vagenasa, T. Karambasa, K. Dimoua, and T. Zarkadasa, "Field Observations of Waves Generated by Passing Ships: A Note," *Coastal Eng.*, vol. 54, pp. 369-375, 2007.

[15] T. Havelock, "The Propagation of Groups of Waves in Dispersive Media, with Application to Waves on Water Produced by a Travelling Disturbance," *Proc. Royal Soc.*, pp. 398-430, 1908.

[16] A.T. Chwang and Y. Chen, "Field Measurement of Ship Waves in Victoria Harbor," *J. Eng. Mechanics*, vol. 129, pp. 1138-1148, 2003.

[17] B. Hubbard and F. Meyer, *The World According to Wavelets: The Story of a Mathematical Technique in the Making*. AK Peters Wellesley, 1996.

[18] Y. Liu, K. Liu, and M. Li, "Passive Diagnosis for Wireless Sensor Networks," *IEEE/ACM Trans. Networking*, vol. 18, no. 4, pp. 1132-1144, Aug. 2010.

[19] G.W. Challen, J. Waterman, and M. Welsh, "IDEA: Integrated Distributed Energy Awareness for Wireless Sensor Networks," *Proc. Eighth Int'l Conf. Mobile Systems, Applications, and Services (MobiSys '10)*, 2010.

[20] K. Wu, H. Tan, Y. Liu, Q. Zhang, and L.M. Ni, "Side Channel: Bits over Interference," *Proc. MobiCom*, 2010.

[21] K. Wu, H. Tan, H. Ngan, and L.M. Ni, "Chip Error Patterns Analysis in IEEE 802.15.4," *Proc. IEEE INFOCOM*, 2010.

[22] T. He, S. Krishnamurthy, J. Stankovic, T. Abdelzaher, L. Luo, R. Stoleru, T. Yan, L. Gu, J. Hui, and B. Krogh, "Energy-Efficient Surveillance System Using Wireless Sensor Networks," *Proc. Second Int'l Conf. Mobile Systems, Applications, and Services (MobiSys '04)*, pp. 270-283, 2004.

[23] P. Dutta, M. Grimmer, A. Arora, S. Bibyk, and D. Culler, "Design of a Wireless Sensor Network Platform for Detecting Rare, Random, and Ephemeral Events," *Proc. Fourth Int'l Symp. Information Processing in Sensor Networks (IPSN '05)*, 2005.

[24] H. Zhu and L.M. Ni, "HERO: Online Real-Time Vehicle Tracking in Shanghai," *Proc. IEEE INFOCOM*, pp. 942-950, 2008.

[25] E. Carapezza, J. Butman, I. Babb, and A. Bucklin, "Sustainable Coastal Sensor Networks: Technologies and Challenges," *Proc. SPIE*, vol. 6963, p. 696309, 2008.
[26] B. Bunin, A. Sutin, G. Kamberov, H. Roh, B. Luczynski, and M. Burlick, "Fusion of Acoustic Measurements with Video Surveillance for Estuarine Threat Detection," *Proc. SPIE*, vol. 6945, p. 694514, 2008.

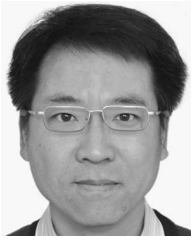

Hanjiang Luo received the BE degree in the Department of Computer Science from Shandong University of Technology and the MS and PhD degrees in the Department of Computer Science, Ocean University of China. His research interests include sensor networks, underwater acoustic networks, Internet of things, and pervasive computing. He is a student member of the IEEE.

Kaishun Wu received the BEng degree from Sun Yat-sen University and the PhD degree in computer science and engineering from Hong Kong University of Science and Technology, in 2007 and 2011, respectively. Currently, he is working as a research assistant professor in Fok Ying Tung Graduate School with the Hong Kong University of Science and Technology. His research interests include wireless communication, mobile computing, wireless sensor networks, and data center networks. He is a member of the IEEE.

Zhongwen Guo received the BE degree in the Department of Computer Science and Engineering from Tongji University, the MS degree in applied mathematics from Ocean University of China, and the PhD degree in detection and processing of marine information from Ocean University of China, in 1987, 1996, and 2005, respectively. Currently, he is with the Department of Computer Science and Technology at Ocean University of China. His research interests include distributed oceanography information processing and network computing. He is a member of the IEEE.

Lin Gu received the BS degree from Fudan University, MS degree from Peking University, and the PhD degree in computer science from the University of Virginia. Currently, he is working as an assistant professor at the Department of Computer Science and Engineering at the Hong Kong University of Science and Technology (HKUST). His research interest includes cloud computing, operating systems, computer networks, and Wireless Sensor Networks (WSNs). He led the development of several novel research systems, including Virtk (a.k.a. t-kernel), the Extended VigilNet, MRlite, and CCMR, a research cloud computing platform. He is a member of the IEEE.

Lionel M. Ni is working as a chair professor in the Department of Computer Science and Engineering at the Hong Kong University of Science and Technology (HKUST). He also serving as the special assistant to the president of HKUST, dean of HKUST Fok Ying Tung Graduate School and visiting chair professor of Shanghai Key Lab of Scalable Computing and Systems at Shanghai Jiao Tong University. He is a fellow of the IEEE.